Asymmetric Multiport Y-Converter for Three-Phase AC Grid Integration with DC Microgrids

Ahmed Y. Farag, Davide Biadene, Tommaso Caldognetto, Paolo Mattavelli
Dept. of Management and Engineering (DTG), University of Padova, Vicenza, Italy
Email: ahmedyahiafarag.abdelfattah@phd.unipd.it, davide.biadene@unipd.it,
tommaso.caldognetto@unipd.it, paolo.mattavelli@unipd.it

***Abstract*—Integration of DC Microgrids (MGs) into distribution networks provides a promising solution to meet the rising demand in the electric energy market. DC MGs offer an efficient solution due to their compatibility with renewable sources, electronic loads, and energy storage. To maintain sustained and reliable operation, DC MGs are commonly connected to utility grids through interlinking converters that can be categorized based on the targeted power levels into single-phase and three-phase converters. With the increasing adoption of small-scale DC MGs for residential and commercial applications, the traditional approach of employing a dedicated converter for each MG can lead to a significant increase in system size and cost. Therefore, the paper introduces multiport converters (MPCs) as a promising alternative consolidating different energy ports. This paper proposes a non-isolated MPC to interface the three-phase AC grid with the 400 V DC MGs. The proposed MPC aims to provide a more compact and efficient power interface. The proposed converter enables a single-stage power conversion among different ports, allowing for potentially enhanced efficiency and power density. The paper provides a thorough analysis of the proposed MPC's operation. Additionally, simulation and experimental validation are presented to demonstrate the converter's performance under different operating conditions.**

***Index Terms*—AC-DC power conversion, Multiport converters, Three-phase inverters, Three-phase rectifiers.**

I. Introduction

DC Microgrids (DC MGs) offer a promising solution to address the growing demand in the electric energy market by connecting distributed power sources to distribution networks. The inherent compatibility of DC MGs with renewable sources, electronic loads, and energy storage allows for more effective and efficient integration of DC sources and loads [1], [2]. Numerous studies have explored the optimal voltage level for low-voltage DC MGs, with the 400 V DC system emerging as the preferred choice for residential and commercial applications [3]. This preference is attributed to its superior overall system efficiency and the requirement for fewer power conversions when connecting multiple energy sources and loads, contributing to sustained and reliable operation. To ensure sustained and reliable operation, DC MGs are commonly linked with utility grids, enabling them to exchange power to maintain power balance within the DC MGs.

Interlinking converters (ICs), connecting 400 V DC MGs with the utility grid, can be categorized based on power levels into single-phase and three-phase ICs. When the IC's power level is limited to a few kilowatts, single-phase ICs are commonly employed. For these single-phase ICs, the two-stage approach is typically adopted to minimize the DC-link capacitance [4]. The first stage involves a single-phase bidirectional converter, while the second stage can incorporate either isolated or non-isolated DC-DC converters. Numerous studies have investigated single-phase ICs, evaluating various combinations of the first and second stage converters in terms of total efficiency, power density, and cost [5].

When targeting higher power levels for the IC, three-phase ICs are utilized. Several single-stage buck-type converters, including the current source converter, the Swiss converter, and the Y-converter, have undergone evaluation [6], [7]. Among these converters, the Y-converter has demonstrated superior overall performance in terms of both efficiency and power density [8]. Additionally, literature discusses two-stage converters formed by connecting a voltage source converter (VSC) in cascade with an additional step-down stage. However, the two-stage solution is less favorable, as the inclusion of an extra power conversion stage and the necessity for intermediate DC link capacitors result in a degradation of the overall efficiency and power density of the IC.

The growing prevalence of DC MGs in residential and commercial applications has prompted a reevaluation of the conventional approach, where a dedicated converter is assigned to each MG for grid interfacing. This traditional method can result in increased system size and costs. Moreover, the use of single-phase ICs may contribute to voltage imbalances in the utility grid due to unequalized loading across the three phases. An efficient and promising alternative to address these challenges is the adoption of multiport converters (MPCs) [9], [10]. MPCs consolidate multiple energy ports into a single hub, offering a more streamlined and cost-effective solution. Fig. 1 depicts the concept of using a single MPC to interface the utility grid with multiple DC MGs.

MPCs not only provide a means to reduce overall size and costs compared to the multi-converter approach but also bring about flexibility and resilience by facilitating direct power flow between different ports. When linking DC MGs with the AC grid, MPCs empower DC MGs to exchange power directly through the converter, reducing reliance on the utility grid. This strategy creates possibilities for optimizing power flow among various energy ports and optimizing the utilization of energy sources and storages in MGs, thereby improving the overall efficiency and reliability of the system.

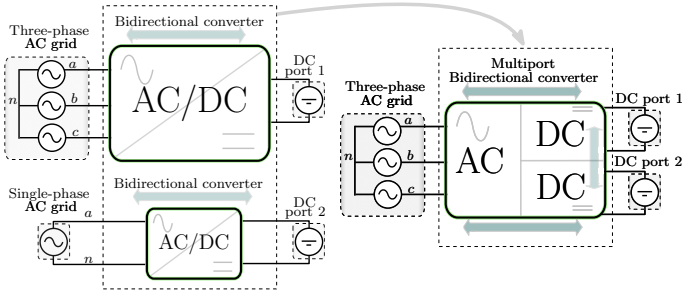

Fig. 1: Multiport converter connecting DC microgrids with the AC grid instead of multiple two-port converters.

In this paper, a non-isolated MPC is proposed to interface the three-phase AC grid with the $400\,\mathrm{V}$ DC MGs. The proposed MPC aims to provide a more compact and efficient power interface by reducing the number of semiconductor devices, passive elements, and EMI filters compared to the multi-converter approach, as presented in Fig.,1. The proposed converter enables a single-stage power conversion among different ports, allowing for potentially enhanced efficiency and power density. Additionally, although designed for the $400\,\mathrm{V}$ DC MGs in this study, the proposed MPC features a buck-boost capability and bidirectional power flow at all ports, providing the flexibility to directly interface with a wide range of DC systems.

The rest of the paper is structured as follows: Sec. II discusses the converter operation and provides a comprehensive analysis of the converter. Sec. III presents the simulation results of the proposed converter. Experimental results are discussed in Sec. IV, and finally, Sec. V provides the conclusion.

II. Principle of Operation and Analysis

The proposed converter builds upon the Y-converter, as introduced in [11], transforming it from a two-port configuration into a multi-port one capable of connecting multiple DC systems to a three-phase AC grid. In its original form, the two-port Y-converter comprised three four-switch buck-boost modules, as demonstrated in Fig. 2a. To develop the multiport converter, the four-switch buck-boost converter is expanded into a six-switch buck-boost converter formed with a shared buck half-bridge and two boost half-bridges. This can be developed in a symmetric or asymmetric configuration. In the symmetric configuration presented in Fig. 2b, the extension from a four-switch to a six-switch buck-boost converter is applied to the three modules. While in the asymmetric configuration presented in Fig. 2c, the extension from a four-switch to a six-switch buck-boost converter is applied only to one of the modules.

The asymmetric multiport Y-converter, denoted as AY-MPC, offers a reduced structure with a lower number of semiconductor devices and inductors compared to the symmetric multiport Y-converter, denoted as Y-MPC. For the presented case study where the two DC systems have different power levels, the AY-MPC enables the integration of the lower power DC system into the three-phase IC with a minimum number of components, allowing for a simpler structure and a compact size. However, a challenge in the AY-MPC is to maintain balanced AC-grid currents, a topic that will be addressed in this section.

In the AY-MPC, similar to the two-port Y-converter, the three modules are interconnected at a central point denoted as m, which functions as the neutral point for the Y-connection of the modules. As each module serves as a DC-DC converter, it is crucial to maintain a non-negative voltage on the AC side of the module ($v_{\{a,b,c\}m} \geq 0\,\mathrm{V}$). To achieve this, an offset voltage is necessary between grid neutral point n and m. A constant offset voltage (V_{off}) is then applied, which should be higher than the peak value of the AC grid phase voltage ($\hat{V}_m$). The AC-side voltages v_{am}, v_{bm}, and v_{cm} can be mathematically expressed as:

$$\begin{aligned} v_{am} &= \hat{V}_m \sin(\omega t) + V_{off} \\ v_{bm} &= \hat{V}_m \sin(\omega t - 2\pi/3) + V_{off} \\ v_{cm} &= \hat{V}_m \sin(\omega t + 2\pi/3) + V_{off} \end{aligned} \tag{1}$$

where ω is the AC grid frequency in rad/s.

The analysis of the converter is presented by considering module a depicted in Fig. 3, while the other modules will remain in the same operation as the two-port Y-converter. Additionally, in the subsequent analysis, it is assumed that at least one of the DC ports' voltage is lower than the peak of the AC side voltage ($\hat{V}_m + V_{off}$), and V_{dc1} is lower than V_{dc2}. Other operation modes, such as when V_{dc2} is lower than V_{dc1}, are not discussed in the article. Module a consists of the two inductors L_1 and L_2 along with three half-bridges: one on the AC side, labeled as $Buck\,a$, and the others on the DC sides, labeled as $Boost\,a1$ and $Boost\,a2$. Based on these assumptions, the $Buck\,a$ and $Boost\,a1$ half-bridges are under control, ensuring that only one of them is modulated at any given moment, while the other remains clamped based on the values of v_{am} and V_{dc1}, whereas $Boost\,a2$ will be modulated continuously.

When v_{am} is greater than V_{dc1}, that is, when $t_1 < t < t_2$, as illustrated in Fig. 4, the $Buck\,a$ half-bridge keeps switching, while the $Boost\,a1$ half-bridge is clamped with S_{a3} on and S_{a4} off. To determine the duty cycle of S_{a1}, denoted as $d_{buck,a}$, the following calculation can be applied:

$$d_{buck,a} = \frac{V_{dc1}}{v_{am}} = \frac{V_{dc1}}{\hat{V}_m \sin(\omega t) + V_{off}} \tag{2}$$

and the duty cycle of S_{a2} is the complementary of $d_{buck,a}$.

For the $Boost\,a2$ half-bridge, it operates with a fixed duty cycle during this period, depending on the ratio between V_{dc1} and V_{dc2}. The duty cycle of S_{a5}, denoted as $d_{boost,a2}$, can be calculated as follows:

$$d_{boost,a2} = \frac{V_{dc1}}{V_{dc2}} \tag{3}$$

and the duty cycle of S_{a6} is the complementary of $d_{boost,a2}$.

The AC grid current of phase a, denoted as i_a, is assumed to be pure sinusoidal and in phase with its corresponding phase

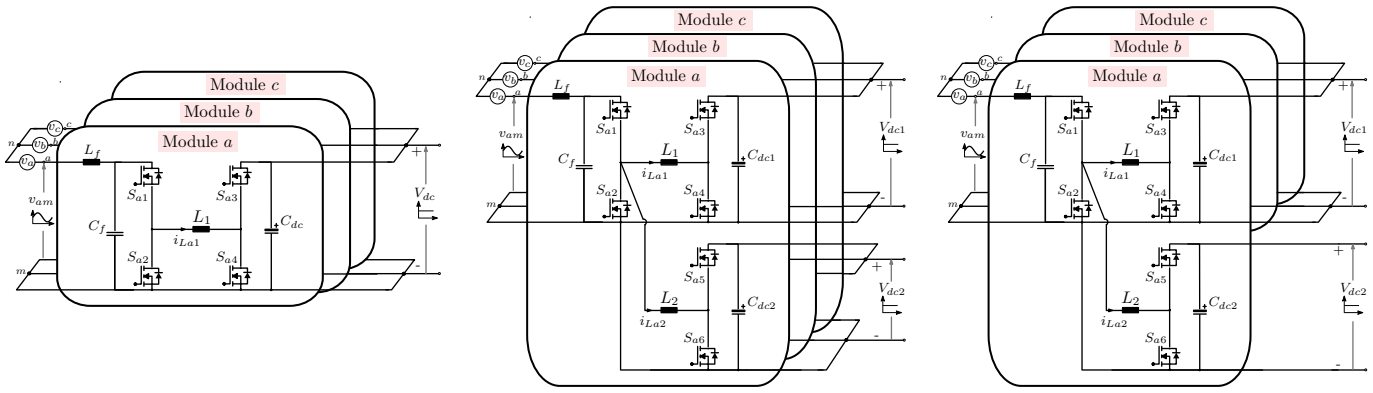

Fig. 2: Different configurations of the modular Y-converter: (a) The two-port Y-converter, (b) The symmetric multiport Y-converter (Y-MPC), and (c) The asymmetric multiport Y-converter (AY-MPC).

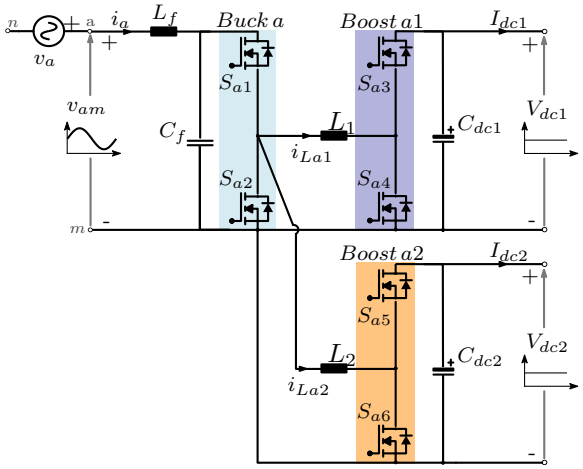

Fig. 3: Module a of the proposed converter.

voltage v_a and then can be calculated as follows:

$$i_a = \hat{I}_m \sin(\omega t) = \frac{2(P_{dc1} + P_{dc2})}{3\hat{V}_m} \sin(\omega t) \tag{4}$$

where P_{dc1} and P_{dc2} represent the power delivered to DC ports 1 and 2, respectively, and $\hat{I}_m$ denotes the peak phase current.

The summation of average inductor currents ($i_{La1,av}$ + $i_{La2,av}$), denoted as $i_{La,av}$, can be derived by applying Kirchhoff's Current Law (KCL) at the AC input of the module, as follows:

$$i_{La,av} = i_{La1,av} + i_{La2,av} = \frac{i_a + i_{Cf,a}}{d_{buck,a}} \tag{5}$$

where $i_{Cf,a}$ represents the current through the input capacitor C_f. By neglecting $i_{Cf,a}$, the equation can be simplified as follows:

$$i_{La,av} = \frac{i_a}{d_{buck,a}} = \frac{\hat{I}_m \sin(\omega t)}{d_{buck,a}} \tag{6}$$

In order to maintain a balanced AC-grid curents, i_{la2} is controlled to deliver the required P_{dc2} to DC port 2 while i_{la1} is controlled to ensure balanced current at the AC grid. Using (6), $i_{la2,av}$ and $i_{la1,av}$ can be determined as follows:

$$\begin{aligned} i_{La2,av} &= \frac{2P_{dc2}}{\hat{V}_m \cdot d_{buck,a}} \sin(\omega t) \\ i_{La1,av} &= \frac{2P_{dc1} - 4P_{dc2}}{3\hat{V}_m \cdot d_{buck,a}} \sin(\omega t) \end{aligned} \tag{7}$$

Similarly, when v_{am} is lower than V_{dc1}, that is, when $0 \leq t \leq t_1$ and $t_2 \leq t \leq T$, the $Boost, a1$ half-bridge keeps switching, while the $Buck, a$ half-bridge is clamped with S_{a1} on and S_{a2} off. To determine the duty cycle of S_{a3}, denoted as $d_{boost,a1}$, the following calculation can be applied:

$$d_{boost,a1} = \frac{v_{am}}{V_{dc1}} = \frac{\hat{V}_m \sin(\omega t) + V_{off}}{V_{dc1}} \tag{8}$$

and the duty cycle of S_{a4} is the complementary of $d_{boost,a}$.

For the $Boost\, a2$ half-bridge, $d_{boost,a2}$, can be calculated as follows:

$$d_{boost,a2} = \frac{v_{am}}{V_{dc2}} = \frac{\hat{V}_m \sin(\omega t) + V_{off}}{V_{dc2}} \tag{9}$$

Using (7) and given that $d_{buck,a} = 1$ in this mode, $i_{la2,av}$ and $i_{la1,av}$ can be determined as:

$$\begin{aligned} i_{La2,av} &= \frac{2P_{dc2}}{\hat{V}_m} \sin(\omega t) \\ i_{La1,av} &= \frac{2P_{dc1} - 4P_{dc2}}{3\hat{V}_m} \sin(\omega t) \end{aligned} \tag{10}$$

The key waveforms for module a of the proposed converter are plotted in Fig. 4. Additionally, the basic characteristic equations of the proposed converters are summarized in Table I where $x = (a, b, c)$.

III. Simulation Results

Simulation results of the proposed converter are presented in Fig. 5 to showcase its performance under different operating conditions, where the power delivered to V_{dc1} is fixed for all

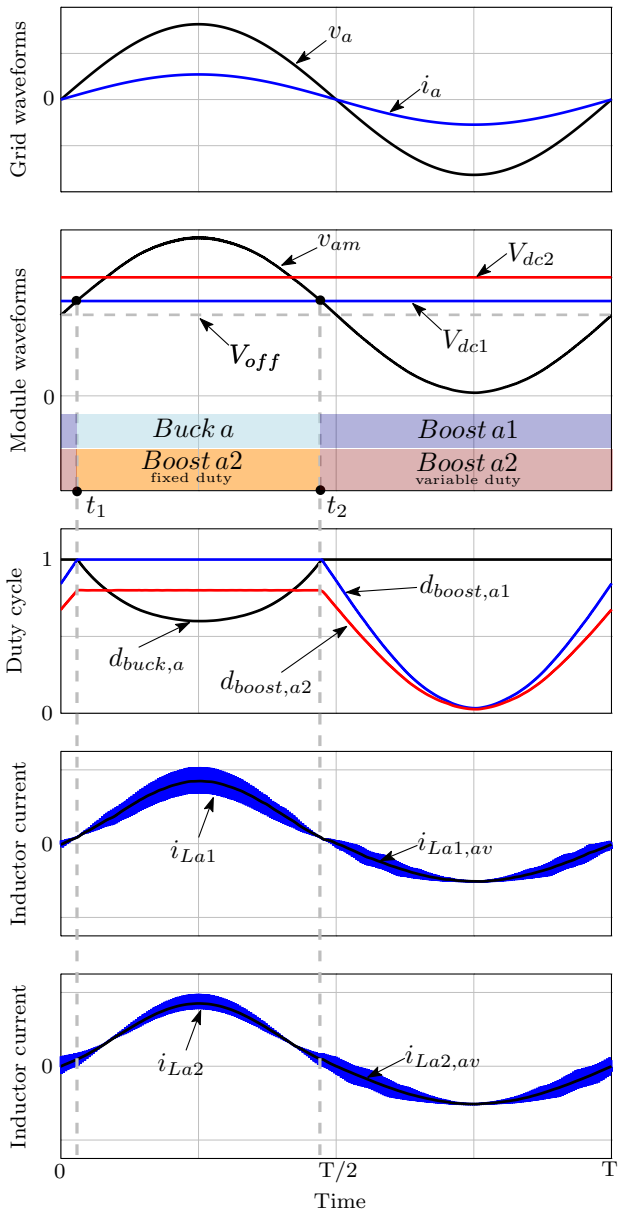

Fig. 4: key waveforms of module a.

tests at 6 kW. The simulations are conducted with the rated voltage at the AC port, while the DC MGs are allowed to have up to a 10% voltage deviation from their rated value. Therefore, in the following simulations, V_{dc1} and V_{dc2} are set equal to 400 V and 440 V, respectively. The converter's specifications are summarized in Table,II.

Three different operating conditions are presented in this section. In the first operating condition, demonstrated in Fig. 5a, the AY-MPC is controlled to deliver no power to V_{dc2} (i.e., P_{dc2} equal to zero). In this case, the converter operates as the conventional two-port Y-converter with zero average current flowing in L_2 (only a high-frequency ripple current) while i_{La1}, i_{Lb1}, and i_{Lc1} remain symmetric.

In Fig. 5b, the second operating condition is presented,

TABLE I: Basic equations of the proposed converter

Parameter	Equation
v_{xm}	$v_x + V_{off}$
$d_{buck,x}$	$\min(1, \frac{V_{dc1}}{v_{xm}})$
$d_{boost,x1}$	$\min(1, \frac{v_{xm}}{V_{dc1}})$
$d_{boost,a2}$	$\frac{\min(v_{am}, V_{dc1})}{V_{dc2}}$
$i_{Lx,av}$	$\frac{i_x}{d_{buck,x}}$
$i_{La1,av}$	$\frac{2P_{dc1} - 4P_{dc2}}{3\hat{V}_m \cdot d_{buck,a}} \sin(\omega t)$
$i_{La2,av}$	$\frac{2P_{dc2}}{\hat{V}_m \cdot d_{buck,a}} \sin(\omega t)$

TABLE II: Parameters of the proposed converter

Parameter	Symbol	Value
Rated AC power	$P_{ac,r}$	9 kW
Rated DC power	$P_{dc1,r}$, $P_{dc2,r}$	6 kW, 3 kW
AC line voltage, frequency	V_{ll}, f_o	400 V, 50 Hz
DC voltage	V_{dc1}, V_{dc2}	360 −440 V
Switching frequency	f_{sw}	62.5 kHz
Inductance	L_1, L_2	330 µH

where P_{dc2} is equal to 1 kW. In this case, i_{La2} is controlled to deliver the required P_{dc2}, while i_{La1} is controlled to maintain balanced AC grid currents. Therefore, i_{La1}, i_{Lb1}, and i_{Lc1} are no longer symmetric, as i_{La1} has a lower amplitude, resulting in a reduced power contribution from module a to P_{dc1} compared to the remaining modules. Despite the asymmetric power flow in the AY-MPC, the AC grid currents remain sinusoidal and balanced, as evident from the simulation results.

Fig. 5c illustrates the third operating condition where P_{dc2} is equal to 3 kW, representing 50% of P_{dc1}. In this case, and as evident from (7) and (10), $i_{La1,av}$ will be zero to maintain balanced AC grid currents. Here, P_{dc1} is divided equally between module b and module c, while module a delivers only P_{dc2}. Once again as evident from the simulation results, the AC grid currents remain sinusoidal and balanced, despite the asymmetric power flow.

IV. Experimental Results

The experimental prototype of the AY-MPC, shown in Fig. 6, is utilized to validate the converter's operation and to confirm the correctness of the presented waveforms. The proposed converter is constructed using four Imperix SIC power modules (PEB8024 with C2M0080120D SiC MOSFETs) for the boost half-bridges and three half-bridges with UF4SC120023K4S SiC MOSFETs. The converter is controlled by a B-box controller from Imperix. Bidirectional AC

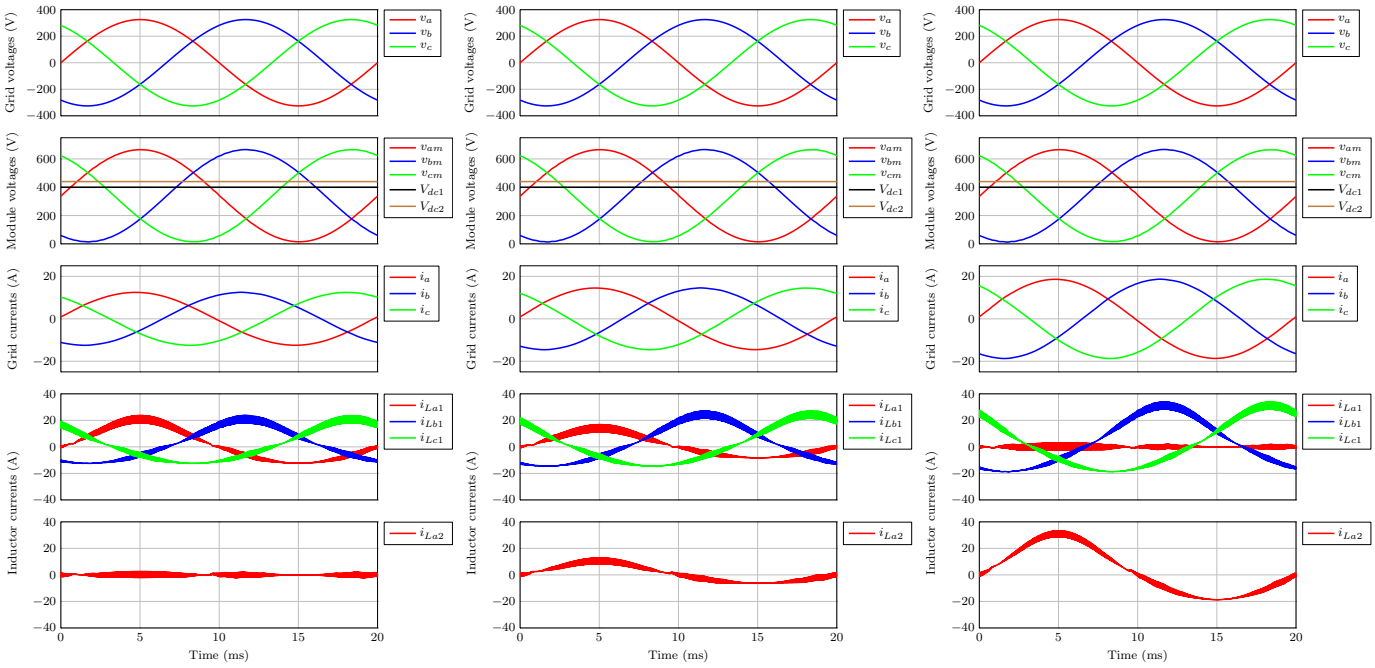

Fig. 5: Simulation results of the proposed converter under P_{dc1} is equal to 6 kW and different values of P_{dc2}: (a) P_{dc2} is equal to 0 kW, (b)P_{dc2} is equal to 1 kW, and (c) P_{dc2} is equal to 3 kW.

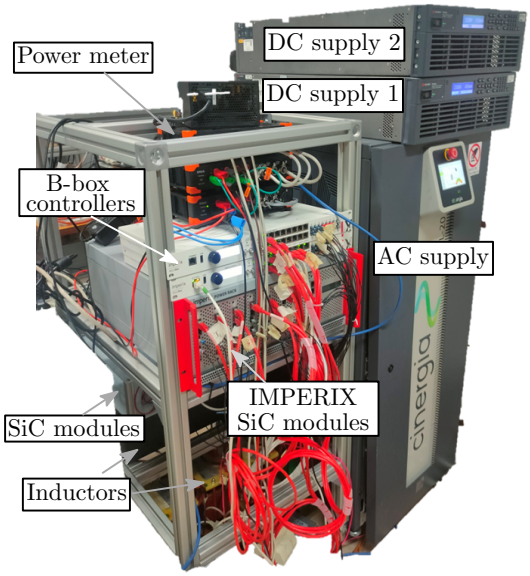

Fig. 6: Picture of the experimental prototype.

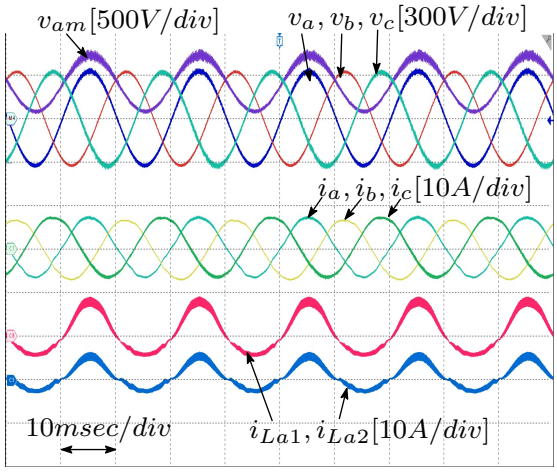

Fig. 7: Experimental waveforms in rectification mode.

and DC power supplies are used to emulate the AC grid and DC microgrids. Additionally, a single-stage input filter is realized with $L_f = 1.2\,\text{mH}$ and $C_f = 10\,\mu\text{F}$, while for L_1 and L_2, 330 µH inductors are used.

Experimental waveforms at steady-state are displayed in Fig. 7, where the converter operates with V_{dc1} and V_{dc2} set to 360 V and 400 V, respectively, and P_{dc1} and P_{dc2} equal to 2.7 kW and 0.5 kW, respectively. The captured waveforms encompass the AC grid voltages (v_a, v_b, v_c), AC-side voltage of module a (v_{am}), the AC grid currents (i_a, i_b, i_c), and the module a inductors' currents (i_{La1}, i_{La2}). As evident from the waveforms, the experimental waveforms match the analysis and simulation results. Additionally, the AC currents are sinusoidal, balanced, and synchronized with the AC voltages.

A contour plot of the measured prototype efficiency is depicted in Fig. 8. To construct this plot, the efficiency measurements of the prototype are recorded while P_{dc1} is swept from 0.3 kW to 2.7 kW with a fixed step of 0.1 kW, and P_{dc2} is swept from 0.15 kW to 0.8 kW with a fixed step of 0.05 kW. The prototype demonstrates a peak efficiency of 94.84%.

The transient behavior of the proposed converter is evalu-

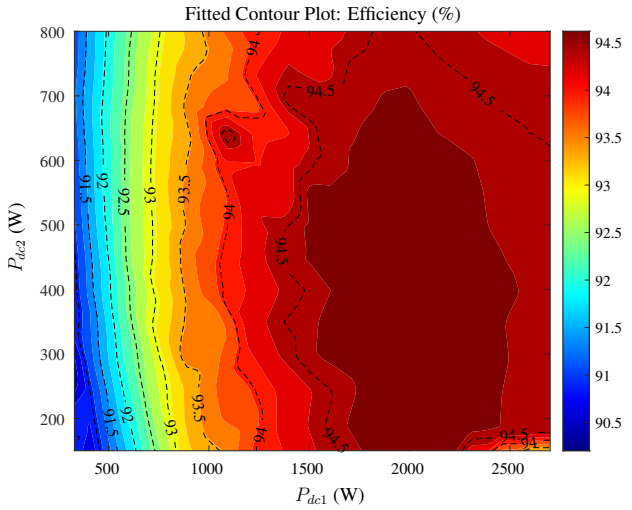

Fig. 8: Contour plot depicting the measured prototype efficiency.

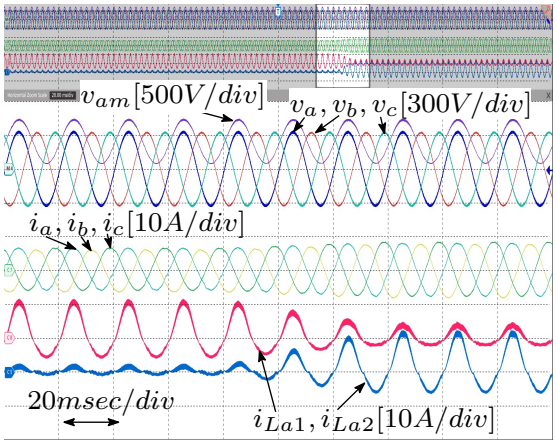

Fig. 9: Experimental waveforms illustrating the transient behavior as P_{dc2} is increased from 0.1 kW to 1 kW, while maintaining a constant P_{dc1}.

ated under power reference variation. In Fig. 9, the converter initially operates in rectification mode with P_{dc1} and P_{dc2} equal to 2.7 kW and 0.1 kW, respectively. P_{dc2} is then increased from 0.1 kW to 1 kW while keeping P_{dc1} constant. The experimental results illustrate the change in i_{La2} to deliver the required P_{dc1} while i_{La1} decreases to maintain a balanced AC current.

V. Conclusion

The integration of DC MGs into distribution networks emerges as a prospective solution to address the growing demand in the electric energy market. Ensuring sustained and reliable operation, DC MGs commonly connect to utility grids through interlinking converters. As the adoption of small-scale DC MGs increases for residential and commercial use, the conventional practice of employing a dedicated converter for each MG becomes impractical due to its potential impact on system size and cost. In light of this, the paper introduces MPCs as a promising alternative that consolidates various energy ports. Specifically, the paper proposes a non-isolated MPC designed to interface the three-phase AC grid with 400 V DC MGs, aiming for a more compact and efficient power interface. This proposed converter enables single-stage power conversion among different ports, offering potential enhancements in efficiency and power density. The paper includes a comprehensive analysis of the proposed MPC's operation, along with simulation and experimental validation to showcase its performance across diverse operating conditions.

Acknowledgment

This work was supported by the European Union's Horizon Europe research and innovation programme in the framework of the project "iPLUG" with grant agreement number 101069770.

References

[1] T. Dragičević, X. Lu, J. C. Vasquez, and J. M. Guerrero, "DC Microgrids—Part II: A Review of Power Architectures, Applications, and Standardization Issues," *IEEE Transactions on Power Electronics*, vol. 31, no. 5, pp. 3528-3549, 2016.

[2] D. Kumar, F. Zare, and A. Ghosh, "DC Microgrid Technology: System Architectures, AC Grid Interfaces, Grounding Schemes, Power Quality, Communication Networks, Applications, and Standardizations Aspects," *IEEE Access*, vol. 5, pp. 12230-12256, 2017.

[3] L. Li, K. -J. Li, K. Sun, Z. Liu and W. -J. Lee, "A Comparative Study on Voltage Level Standard for DC Residential Power Systems," *IEEE Transactions on Industry Applications*, vol. 58, no. 2, pp. 1446-1455, 2022.

[4] D. Dong, I. Cvetkovic, D. Boroyevich, W. Zhang, R. Wang, and P. Mattavelli, "Grid-Interface Bidirectional Converter for Residential DC Distribution Systems—Part One: High-Density Two-Stage Topology," *IEEE Transactions on Power Electronics*, vol. 28, no. 4, pp. 1655-1666, 2013.

[5] M. Alshammari and M. Duffy, "Review of Single-Phase Bidirectional Inverter Topologies for Renewable Energy Systems with DC Distribution," *Energies*, vol. 15, no. 18, article number 6836, 2022.

[6] L. Schrittwieser, M. Leibl, M. Haider, F. Thöny, J. W. Kolar and T. B. Soeiro, "99.3% Efficient Three-Phase Buck-Type All-SiC SWISS Rectifier for DC Distribution Systems," *IEEE Transactions on Power Electronics*, vol. 34, no. 1, pp. 126-140, 2019.

[7] A. Y. Farag, D. Biadene, P. Mattavelli, and T. Younis, "Three-phase Four-wire Bidirectional Y-converter for an Enhanced Interface between the AC Grid and the Unipolar DC Microgrid," *2023 8th IEEE Workshop on the Electronic Grid (eGRID)*, pp. 1-6, 2023.

[8] A. Y. Farag, T. Younis, D. Biadene, and P. Mattavelli, "AC Grid-DC Microgrid Coupling with High-Performance Three-Phase Single-Stage Bidirectional Converters," *Energies*, vol. 16, no. 17, article number 6106, 2023.

[9] A. K. Bhattacharjee, N. Kutkut, and I. Batarseh, "Review of Multiport Converters for Solar and Energy Storage Integration," *IEEE Transactions on Power Electronics*, vol. 34, no. 2, pp. 1431-1445, Feb. 2019.

[10] Z. Huang, D. Zhou, L. Wang, Z. Shen and Y. Li, "A Review of Single-Stage Multiport Inverters for Multisource Applications," *IEEE Transactions on Power Electronics*, vol. 38, no. 5, pp. 6566-6584, May 2023

[11] M. Antivachis, N. Kleynhans, and J. W. Kolar, "Three-Phase Sinusoidal Output Buck-Boost GaN Y-Inverter for Advanced Variable Speed AC Drives," *IEEE Journal of Emerging and Selected Topics in Power Electronics*, vol. 10, no. 3, pp. 3459-3476, 2022.